



OPEN

Oleuropein confers neuroprotection against rotenone-induced model of Parkinson's disease via BDNF/CREB/Akt pathway

Richa Singh, Walia Zahra, Saumitra Sen Singh, Hareram Birla, Aaina Singh Rathore, Priyanka Kumari Keshri, Hagera Dilnashin, Shekhar Singh & Surya Pratap Singh

Major pathological features of Parkinson's disease (PD) include increase in oxidative stress leading to the aggregation of α -synuclein, mitochondrial dysfunction and apoptosis of dopaminergic neurons. In addition, downregulation of the expression of neurotrophic factors like-Brain Derived Neurotrophic Factor (BDNF) is also involved in PD progression. There has been a lot of interest in trophic factor-based neuroprotective medicines over the past few decades to treat PD symptoms. Rotenone, an insecticide, inhibits the mitochondrial complex I causing overproduction of ROS, oxidative stress, and aggregation of α -synuclein. It has been shown that BDNF and Tropomyosin receptor kinase B (TrkB) interaction initiates the regulation of neuronal cell development and differentiation by the serine/threonine protein kinases like Akt and GSK-3 β . Additionally, Transcription factor CREB (cAMP Response Element-binding protein) also determines the gene expression of BDNF. The homeostasis of these signalling cascades is compromised with the progression of PD. Therefore, maintaining the equilibrium of these signalling cascades will delay the onset of PD. Oleuropein (OLE), a polyphenolic compound present in olive leaves has been documented to cross blood brain barrier and shows potent antioxidative property. In the present study, the dose of 8, 16 and 32 mg/kg body weight (bwt) OLE was taken for dose standardisation. The optimised doses of 16 and 32 mg/kg bwt was found to be neuroprotective in Rotenone induced PD mouse model. OLE improves motor impairment and upregulate CREB regulation along with phosphorylation of Akt and GSK-3 β in PD mouse. In addition, OLE also reduces the mitochondrial dysfunction by activation of enzyme complexes and downregulates the proapoptotic markers in Rotenone intoxicated mouse model. Overall, our study suggests that OLE may be used as a therapeutic agent for treatment of PD by regulating BDNF/CREB/Akt signalling pathway.

Abbreviations

PD	Parkinson's disease
OLE	Oleuropein
NTs	Neurotrophins
BDNF	Brain derived neurotrophic factor
CREB	CAMP response element-binding protein
SNpc	Substantia Nigra Pars Compacta
TH	Tyrosine hydroxylase
ROS	Reactive oxygen species
DA	Dopaminergic neurons
SOD	Superoxide Dismutase
Ca ²⁺	Calcium

Parkinson disease (PD) is the most prevalent neurodegenerative condition and movement disorder. The word parkinsonism refers to complex symptom that includes resting tremor, bradykinesia, and muscular stiffness^{1,2}. The motor symptoms of PD are related to the degeneration of dopaminergic neurons (DA) in substantia nigra

Department of Biochemistry, Institute of Science, Banaras Hindu University, Varanasi, UP 221005, India. email: suryasinghbhu16@gmail.com

pars compacta (SNpc) and reduction of dopamine in striatum of mesencephalon. Although the existence of non-motor symptoms such as constipation, depression, sleep difficulties and cognitive impairment can also suggest neuronal loss in non-dopaminergic regions^{3,4}. In persons 60 years and older, the prevalence of PD is estimated to be around 1%, rising from 1 to 3% in those aged 80 and above⁵. However, it is crucial to note that these figures do not include undiagnosed cases. The incidence of PD differs by gender, with a 3:2 ratio of males to females, with a delayed beginning in females attributable to neuroprotective action of estrogen on the nigrostriatal dopaminergic pathway⁶. Several cellular signalling pathways have been linked to the development of PD, with α -synuclein aggregation adopting a β -sheet-rich amyloid-like form being key to the progression of disease⁷. Previous studies have suggested that aberrant protein clearance, mitochondrial dysfunction, oxidative stress and neuroinflammation are all implicated in the genesis and progression of PD^{8,9}. Brain-derived neurotrophic factor (BDNF), one of the neurotrophins (NTs) is involved in physiological function of the central nervous system (CNS). BDNF affects neuronal cell differentiation, survival, and neurite outgrowth of dopaminergic neurons, which is important for nervous system development^{10,11}. It interacts with its major ligand TrkB through the immunoglobulin constant 2 (Ig-C2) domain, and this complex promotes neuronal survival by activating various downstream cascades via the phosphatidylinositol 3-kinase/Akt (PI3K/Akt) signalling pathways¹². Akt is a major downstream kinase protein in BDNF/TrkB signalling which involved in neuronal cell survival¹³. When BDNF binds to the TrkB receptor, Akt is activated, while GSK-3 is deactivated due to phosphorylation at ser9, promoting cell survival. Activated Akt is also needed to phosphorylate CREB (cAMP Response Element-binding protein) at ser133 and convert it to its active form^{14,15}. The BDNF gene contains CREB-binding sequences. CREB might be upstream of BDNF and upregulate BDNF expression. The survival, development, and synaptic plasticity of neurons are all affected by these cascades¹⁶.

Several investigations have shown that BDNF/TrkB signalling is involved in PD and have evaluated the possible therapeutic use of BDNF. TrkB is widely distributed in dopaminergic neurons of nigrostriatal region. Dopaminergic neuronal death is connected to pathogenic α -synuclein mutations that alter the interaction of BDNF with its receptor TrkB^{17,18}. TrkB lipid raft distribution is suppressed by α -Synuclein, which also inhibits internalisation and axonal trafficking. α -Synuclein also inhibits TrkB production by binding with its kinase domain and causing its ubiquitination¹⁹. Therefore, reduced expression of BDNF and TrkB due to increase in oxidative stress and alpha synuclein aggregation was observed in PD²⁰. Reduced p-Akt/Akt ratio is seen in the dopaminergic neurons of post-mortem PD brains, which is associated with PI3K/Akt signalling dysregulation and PD pathogenesis²¹. Degeneration of dopaminergic neurons by downregulation of BDNF, TrkB and Akt results in reducing the phosphorylation of CREB²². Thus, the activation of BDNF/CREB/Akt signalling may be studied to observe the neuroprotection against PD. Elevation of calcium (Ca^{2+}) level also contribute to the oxidative stress-mediated PD leading to the α -synuclein aggregation^{23,24}. Neurotrophic BDNF may be helpful in decreasing the expression of a proapoptotic member of this family of proteins like Bax, Caspase3 and promote neuronal cell survival^{25,26}.

Rotenone is a neurotoxin that inhibits mitochondrial electron transport chain (ETC) complex I and induces a parkinsonian like symptoms. It is being frequently used to study the behavioural features and molecular mechanisms of α -synuclein aggregation and degeneration of nigrostriatal dopaminergic neurons^{27,28}. Currently number of drugs that are being used for the treatment of PD have several side effects. Therefore, novel treatment methods are required which can prevent the neuronal cell death and dysfunction. Therefore, natural plants and their structural analogue can serve as a principal source for the identification of novel drug for the treatment of PD²⁹. Polyphenols in plants and fruits have been found to have antioxidant properties which prevents oxidative stress³⁰. Polyphenols are abundant in olives and olive products³¹. The phenolic compound OLE is found in the olive leaf, oil, and fruit in large amounts³². OLE has almost 400% greater antioxidant capacity than vitamin C and double the antioxidant capacity of green tea or grape seed extract, and it may also pass the blood-brain barrier³³. OLE has been shown to have anti-oxidative property in SN of the dopaminergic neurons in rats, as well as against 6-OHDA-induced PC12 cell damage³⁴. In recent years many natural compounds have been shown to protect the degeneration of dopaminergic neurons via PI3K/Akt signalling pathway³⁵. One possible challenge to find a significant dose for observing the neuroprotective effect of OLE through dose standardisation. In our experiment, the different concentration of OLE for dose standardisation was considered from Amira M. Badr et al. method³⁶. OLE dosages of 16 mg/kg and 32 mg/kg bwt were both found to be significant. However, 16 mg/kg bwt was chosen for the subsequent research since it was the lowest dose demonstrating the best outcome.

As BDNF-CREB signalling pathway plays an important role in PD pathogenesis, therefore, this pathway can be targeted for therapeutic treatment of PD. OLE has been known to prevent the degeneration of neuron however, its interaction with different signalling pathways is still unknown. Hence, the present study was aimed to evaluate the neuroprotective effect of OLE on the neuronal growth and survival in rotenone induced parkinsonian mouse model via BDNF/CREB pathway.

Dose chase experiment for the analysis of neuroprotective action of OLE

Results 1. *OLE significantly mitigated motor impairment in Rotenone-induced parkinsonian mouse model.* The observation of narrow beam walking test suggested that Rotenone intoxicated mice had a longer time to cross the beam ($p < 0.001$) as compared to control mice. While the treatment of OLE has significantly improved the behavioural abnormalities than Rotenone intoxicated PD mice model and took less time to cross the beam. Three doses of OLE (viz 8 mg/kg, 16 mg/kg and 32 mg/kg) were taken in the study. 16 mg/kg and 32 mg/kg bwt., doses of OLE were found to be significant ($p < 0.001$) (Fig. 1A). The Data are expressed in terms of mean \pm SEM.

In the case of hanging test, the muscles strength and gripping power in Rotenone induced mice was significantly ($p < 0.001$) less than control group. Whereas in Rotenone group treated with OLE (16 mg/kg and 32 mg/

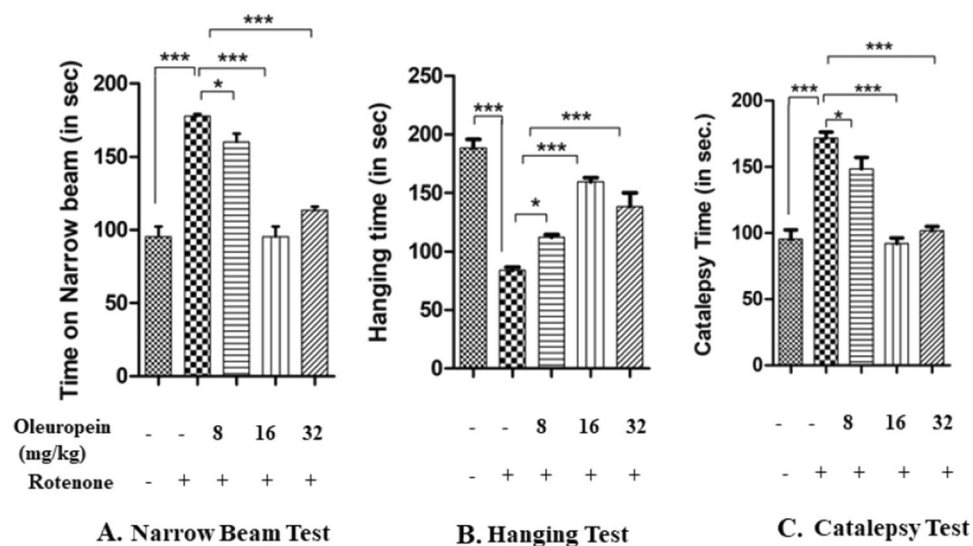


Figure 1. Effect of different doses of OLE on behavioural parameters in rotenone-induced mouse model. Narrow Beam Test showed increase in narrow beam walking time in rotenone group ($***p < 0.001$) as compared to the control group. Whereas, after the treatment with OLE (16 and 32 mg/kg bwt), the walking time of mice to cross the beam was significantly decreased ($***p < 0.001$). Hanging test presented decrease in hanging time in rotenone intoxicated mice as compared to control ($***p < 0.001$) whereas, in OLE treated group (16 and 32 mg/kg bwt), hanging time was significantly reduced ($***p < 0.001$). Catalepsy Test exhibited the reduced latency time to change its unusual posture was associated with rotenone induced mice ($***p < 0.001$) than control. While, significant decrease in catalepsy was observed in OLE treated mice (16 and 32 mg/kg bwt) ($***p < 0.001$). In all these three behavioural parameters, the OLE doses of 8 mg/kg bwt. showed a less significant effect. ($*p < 0.05$). The one-way ANOVA was used to analyse the data, followed by the Newman-Keuls test. The mean \pm SEM ($n = 6$) is used to depict the values.

kg body weight) showed a beneficial effect ($p < 0.001$) towards gripping strength. The group treated with 8 mg/kg OLE show less improvement in motor deficits as compared to rotenone intoxicated group ($p < 0.05$) (Fig. 1B).

The Catalepsy test was performed to check the muscle stiffness. An increase in muscle stiffness was observed ($p < 0.001$) in rotenone-induced mice compared to control. The holding time in the treatment group (16 mg/kg and 32 mg/kg body weight) mice was significantly lower ($p < 0.001$) than rotenone intoxicated group. The observation of 8 mg/kg OLE with rotenone group was relatively less significant ($p < 0.05$) (Fig. 1C). All data are expressed in terms of mean \pm SEM.

Biochemical analysis. *OLE reduces the lipid peroxidation in rotenone intoxicated mice model.* The high level of MDA was observed in rotenone group as compared to control mice. The group treated with OLE of 16 mg/kg and 32 mg/kg bwt showed the significant decrease ($p < 0.001$) in level of MDA. When three different dosages of OLE, (8 mg/kg, 16 mg/kg and 32 mg/kg bwt) were given to the rotenone-induced mice, 16 mg/kg and 32 mg/kg body weight were shown to be more effective than the 8 mg/kg body weight group ($p < 0.05$) (Fig. 2A).

OLE influences the activity of antioxidants. The results showed that the activity of SOD enzyme was reduced ($p < 0.001$) in rotenone administrated mice than control group. Rotenone treated with OLE group (specifically in 16 mg/kg and 32 mg/kg body weight) showed significant increase in the activity of SOD ($p < 0.001$). Likewise, the level of catalase enzyme was significantly reduced ($p < 0.001$) in rotenone induced mice in comparison with control group and optimum catalase activity was seen in groups of 16 mg/kg and 32 mg/kg OLE ($p < 0.001$) (Fig. 2B,C).

Immunohistochemistry analysis. *OLE protects loss of SNpc DA neurons from rotenone-induced PD mice and also reduces the loss of striatal DA at nerve terminals.* The expression of TH in DA neurons in the SN and Striatum (ST) areas of the mouse brain was studied using immunostaining with significant findings between the rotenone groups and OLE treated mice viz. 8 mg/kg, 16 mg/kg and 32 mg/kg body weight. In SN region, rotenone intoxication significantly reduced ($p < 0.001$) the immunoreactivity of TH when compared to control group. The most significant results were obtained in 16 mg/kg and 32 mg/kg bwt ($p < 0.001$ and $p < 0.001$) as compared to 8 mg/kg bwt ($p < 0.05$) (Fig. 3A). Similarly in ST, rotenone administration cause decrease ($p < 0.001$) in immunoreactivity than control group whereas, OLE with doses 16 mg/kg and 32 mg/kg bwt ($p < 0.01$ and $p < 0.001$) showed increase in immunoreactivity than the PD group whereas, OLE with 8 mg/kg bwt had less significant immunoreactivity (Fig. 3B).

Although both 16 mg/kg and 32 mg/kg bwt doses of OLE were found to be significant, nevertheless, the minimum effective dose of 16 mg/kg bwt was taken for further study.

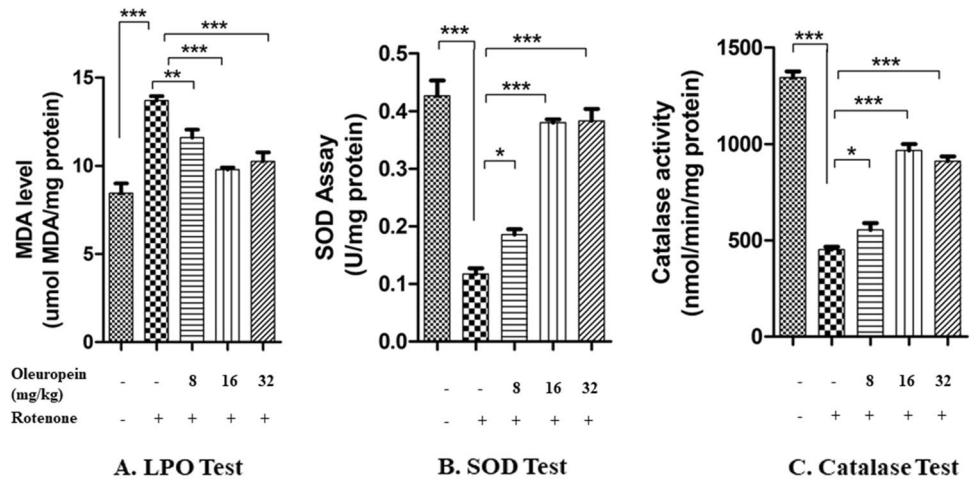


Figure 2. In LPO test, MDA level was elevated in rotenone group as compared to control ($***p < 0.001$) and decreased in case of OLE treated groups notably in 16 and 32 mg/kg bwt. The SOD and Catalase activity was reduced in case of rotenone than control while in OLE treatment (16 and 32 mg/kg bwt), the SOD and Catalase activity was significantly increased. In all these three biochemical parameters, the OLE doses of 8 mg/kg bwt. showed a less significant effect. ($*p < 0.05$). The mean \pm SEM ($n = 6$) is used to depict the values.

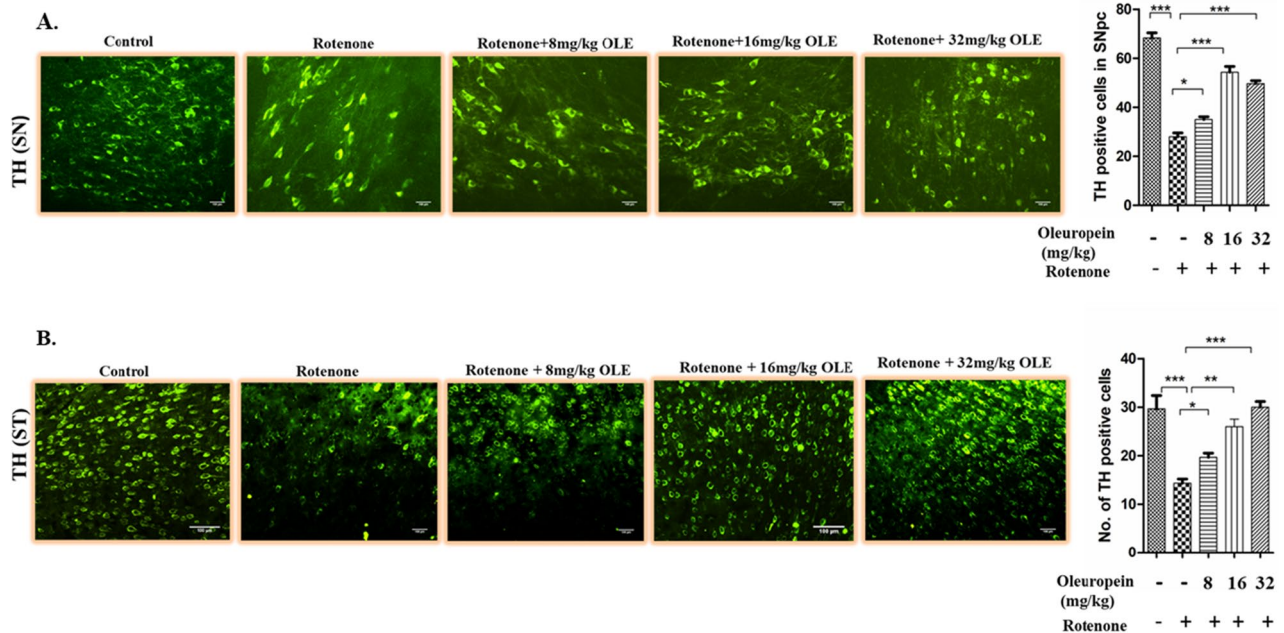


Figure 3. The immunoreactivity of TH in the SN and ST of various experimental groups was examined using immunohistochemistry under the fluorescence microscope (20 \times). Rotenone intoxicated group showed less immunoreactivity than control ($p < 0.001$) in SN and ST. While, increased immunoreactivity of TH was observed in case of OLE treated group (16 and 32 mg/kg bwt) in SN ($p < 0.001$) and ST ($p < 0.01$). In all these three biochemical parameters, the OLE doses of 8 mg/kg bwt. showed a less significant effect. ($*p < 0.05$). Values are expressed as mean \pm SEM ($n = 6$). $***p < 0.001$, and $*p < 0.05$. SEM Standard error of mean, OLE Oleuropein, SN Substantia nigra, TH Tyrosine hydroxylase.

Effect of OLE on neuronal survival in rotenone-intoxicated parkinsonian mouse model

Result 2. *OLE alleviates the mitochondrial ETC chain dysfunction in rotenone-induced PD mice.* Results showed that OLE had an influence on the mitochondrial dysfunction produced by rotenone intoxication. In our investigation, we found that Rotenone along with inhibiting complex I also inhibits the activity of other ETS complexes. Mechanistically, in comparison to rotenone-intoxicated PD mice, OLE treated group showed reduced mitochondrial impairment and enhanced respiratory chain Complex I ($p < 0.001$; Fig. 4A), IV ($p < 0.001$;

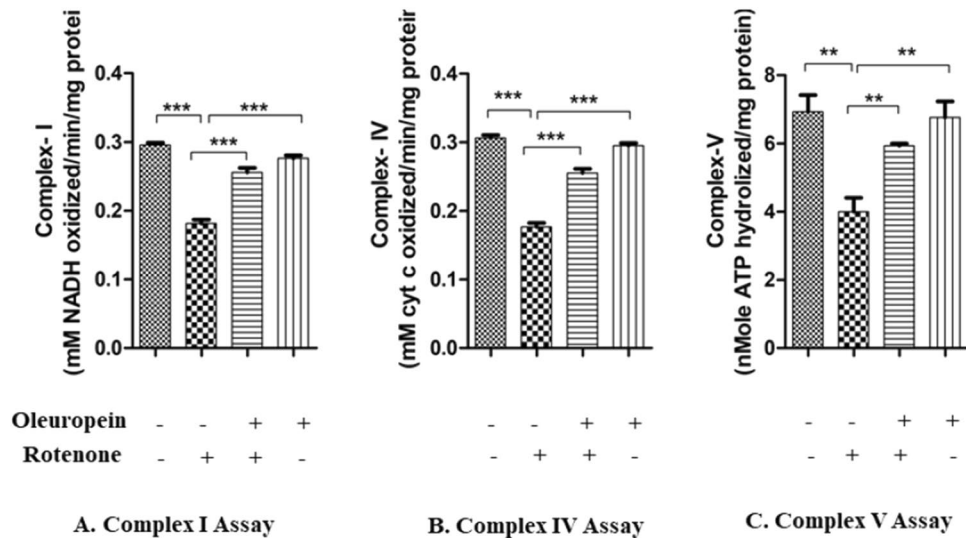


Figure 4. Effect of OLE on mitochondrial complex activity of I, IV and V was observed. In Rotenone-intoxicated mouse brains, the complex activity of I, IV and V was decreased than control whereas in OLE treatment group, significantly increased mitochondrial complexes activity of I, IV and V was observed. The results are provided as mean SEM (n = 5). **p < 0.01, and ***p < 0.001. The mean ± SEM (n = 6) is used to depict the values.

Fig. 4B), and V (p < 0.01; Fig. 4C) activity. There was a substantial decrease in the activity of complexes I (p < 0.001), complex IV (p < 0.001), and complex V (p < 0.01) in rotenone group as compared to control.

OLE reduced the elevated Ca²⁺ level in nigrostriatal region of PD mice. Ca²⁺ levels in the nigrostriatal tissue of PD mice were found to be substantially greater than in control mice (p < 0.001). While OLE treatment led to significant decrease in Ca²⁺ level (p < 0.001) as compared to rotenone-intoxicated groups (Fig. 5).

OLE reduced the apoptotic markers in rotenone-induced PD model. The impact of OLE on proapoptotic (Bax, Caspase3) and antiapoptotic factor (Bcl-2) were examined in PD mice (Fig. 9A). The Bax/Bcl-2 ratio in Rotenone group was considerably higher (p < 0.01) than the control group, and lower in the OLE-treated PD mice (p < 0.01; Fig. 9B), demonstrating the antiapoptotic function of OLE in the parkinsonian mouse model. Similarly, cleaved caspase-3 also get upregulated which supports the increased (p < 0.001) expression of caspase-3 in case of rotenone group as compared to control whereas in OLE administrated group, it was significantly reduced (p < 0.01; Fig. 9C).

OLE enhanced the interaction of BDNF and TrkB by alleviating the aggregation of α-synuclein. It was shown that α-synuclein suppresses BDNF expression and interacts directly with TrkB receptors (as explained above)

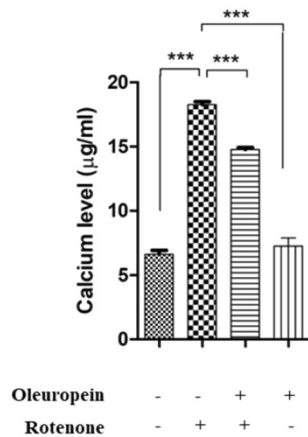


Figure 5. Effect of OLE on Ca²⁺ levels. Rotenone administrated group showed increase in Ca²⁺ levels (***p < 0.001) than control. Additionally in OLE-treated group, significantly reduced Ca²⁺ level was found (***p < 0.001). The results are provided as mean SEM (n = 6),

(Fig. 8A). Hence, decrease in the ratio of p-TrkB/TrkB was seen in rotenone ($p < 0.01$) as compared to control whereas after treatment with OLE, it was significantly enhanced ($p < 0.01$; Fig. 8C) among parkinsonian mice group. Similarly, less immunoreactivity of TrkB in SNpc region was seen in rotenone administrated group ($p < 0.001$) than control group while OLE mitigates the TrkB expression ($p < 0.01$; Fig. 6B). Moreover, the decrease in expression and immunoreactivity of BDNF was observed in PD mice ($p < 0.001$) (Fig. 7B; $p < 0.001$; Fig. 8B) respectively and there was prominent elevation in expression and immunoreactivity of BDNF in OLE treated group ($p < 0.01$). In terms of α -synuclein expression, the rotenone group exhibited substantially more aggregation than the control group ($p < 0.001$) and significantly reduced aggregation was seen in case of OLE treated group ($p < 0.001$; Fig. 8F). In addition, increase in immunoreactivity of α -synuclein was found in SNpc region of rotenone-induced mice ($p < 0.001$) in comparison with control, whereas treatment with OLE showed significant reduction in the immunoreactivity ($p < 0.01$; Fig. 6A).

Effect of OLE on rate-limiting enzyme TH in PD mice. Reduced expression of TH was seen in nigrostriatal region of rotenone intoxicated group ($p < 0.001$). While it was highly upregulated in OLE treated group ($p < 0.001$) in comparison with PD mice (Fig. 8E). These finding suggests that OLE helps in regulating the expression of rate limiting enzyme in parkinsonian mice model.

OLE ameliorates the expression of CREB and phosphorylation of kinases, Akt and GSK-3 β . OLE promoted the neuronal survival gene by modulating the multitarget kinases, Akt and GSK-3 β dysregulation. Rotenone group had a lower ratio of p-Akt/Akt ($p < 0.01$) than control, and the treatment group had a significantly higher p-Akt/Akt ratio ($p < 0.01$; Fig. 9D). Recent research has connected GSK-3 β to intrinsic apoptosis in mitochondria and the activation of CREB. The ratio of p-GSK-3 β /GSK-3 β was declined in rotenone intoxication ($p < 0.001$) whereas it was highly ameliorated in OLE administrated group ($p < 0.01$) (Fig. 9E). Similarly, IHC was done to further support the findings, and the results showed a significant drop ($p < 0.001$) in GSK-3 β phosphorylation among PD group as compared to the control group while the effect of OLE treatment showed increase in GSK-3 β phosphorylation ($p < 0.01$; Fig. 7A). In addition, OLE induced the phosphorylation of CREB by increasing the ratio of these kinases. Hence, the ratio of p-CREB/CREB was increased significantly in OLE administrated group ($p < 0.01$) and decreased in diseased condition ($p < 0.01$; Fig. 8D).

Discussion

The survival of neurons is maintained by a complex interconnected network of signalling cascade that can be disrupted by a variety of cellular stressors. A change in the balance of signalling pathways in response to stress or illness can have dramatic ramifications on growth and differentiation of neuronal cells^{37,38}. This causes

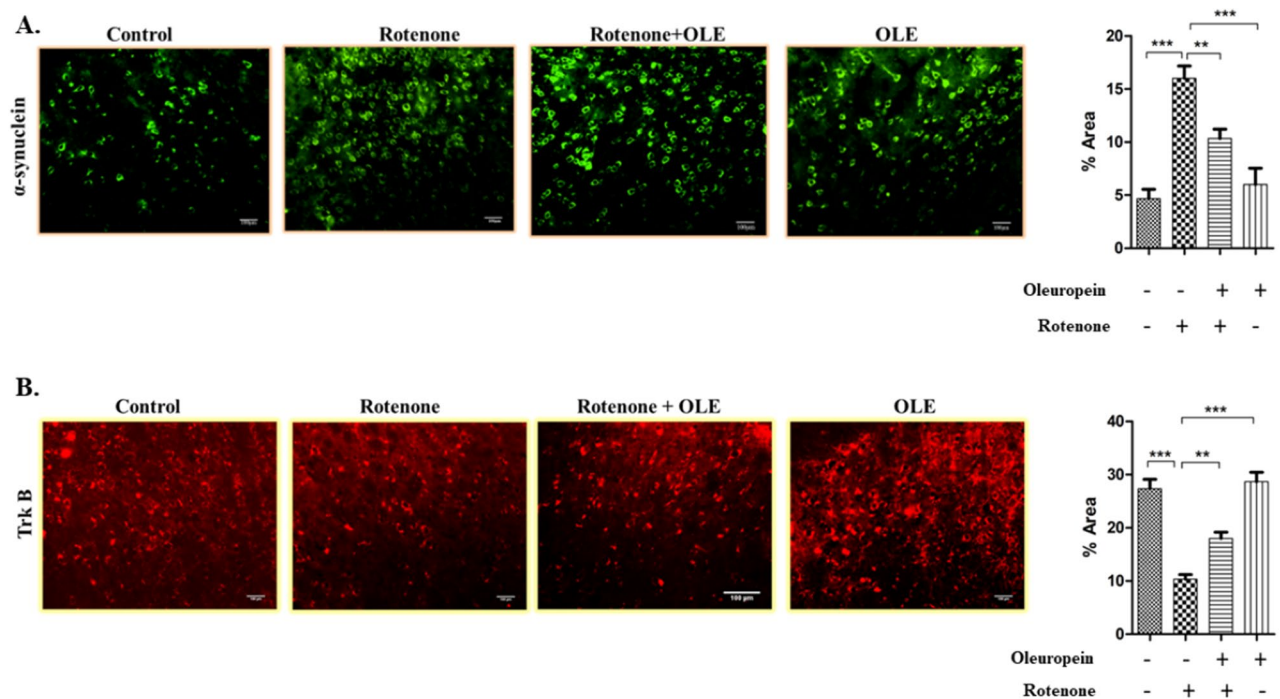


Figure 6. The immunohistochemical staining of (A) α -synuclein and (B) Trk B. The increase in expression of α -synuclein in rotenone group ($***p < 0.001$) while neuroprotection of OLE significantly decreased the expression of α -synuclein ($**p < 0.01$). Similarly, Trk B expression was reduced upon rotenone intoxication ($***p < 0.001$) whereas, OLE significantly upregulated the expression of Trk B in OLE treated group ($**p < 0.01$). The one-way ANOVA was used to analyse the data, followed by the Newman–Keuls test. The mean \pm SEM ($n = 6$) is used to depict the values.

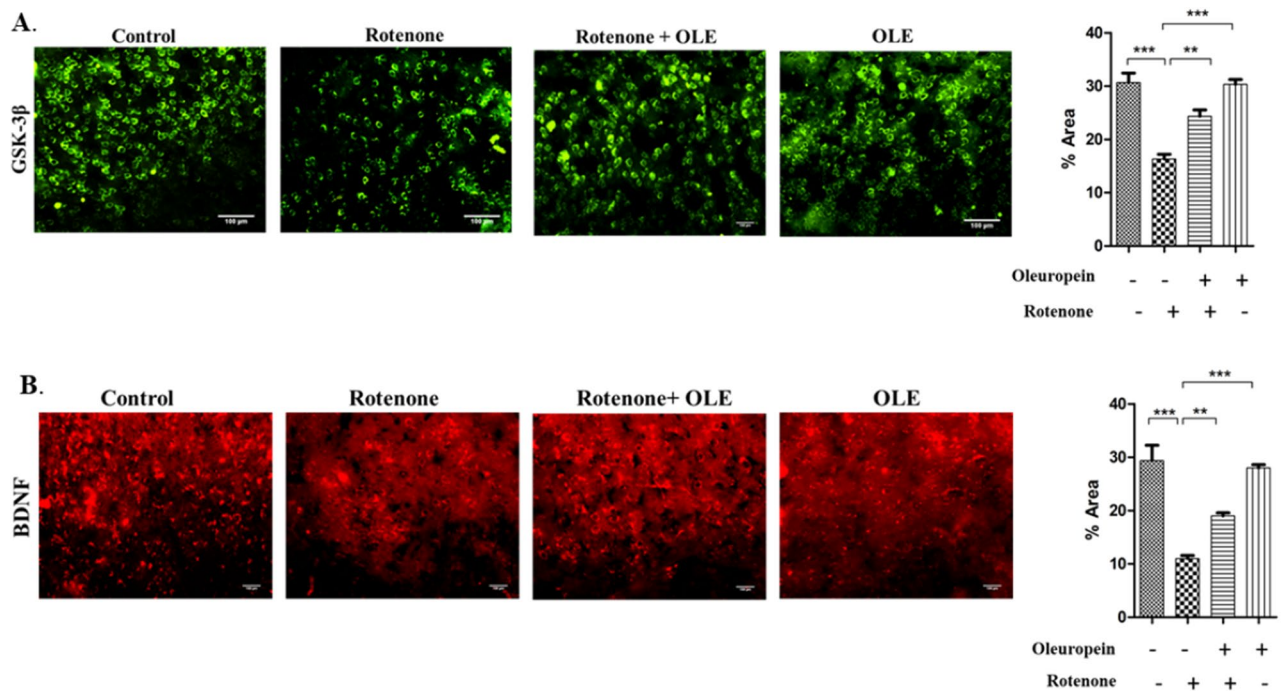


Figure 7. In comparison with the control, immunohistochemical labelling of (A) p-GSK-3 β and (B) BDNF in SN region different experimental groups revealed a reduction in expression in the rotenone group (** $p < 0.001$), whereas OLE treatment dramatically increased p-GSK-3 β and BDNF expression (** $p < 0.01$). The fluorescent image was analysed by software image J at 20 \times magnification. The one-way ANOVA was used to analyse the data, followed by the Newman–Keuls test. The mean \pm SEM ($n = 6$) is used to depict the values.

compromised mitochondrial structure, energy metabolism, and nuclear integrity^{39,40}. These processes are primarily regulated by one of the most important neurotrophic factors such as BDNF, which is important for dopaminergic neuronal survival, plasticity, and differentiation⁴¹. PD is a chronic and progressive disease; its symptoms worsen with time. Current PD medications are symptomatic, necessitating the finding of potent neuroprotectants with fewer side effects⁴². We investigated the efficacy of OLE in rotenone model of Parkinson's disease and found that it reduced the pathological and phenotypic characteristic of PD. OLE promotes the survival, growth and differentiation of dopaminergic neurons through its anti-oxidative and anti-aggregative effects⁴³. Our study, reveals the dynamic changes in the cascade of signalling proteins which are directly related to the degeneration of dopaminergic neurons through Akt/CREB/BDNF pathway. We have also observed the reduced ROS production, mitochondrial dysfunction and apoptosis by OLE in Rotenone induced mice model as shown in Fig. 10.

The findings of our study are consistent with those of previous investigations which have indicated that OLE exhibits a neuroprotective role against chronic stress, induced in parkinsonian mice model. In dose standardisation study we evaluated the effect of different concentration of OLE i.e. 8, 16 and 32 mg/kg bwt on rotenone induced mouse model of PD.

It was observed that mice intoxicated with rotenone showed motor impairment, including prolonged narrow beam walking, reduced hanging time and catalepsy duration. While, administration of 16 and 32 mg/kg bwt of OLE, results in the reduction of latency time in the narrow beam test as well as an increase in hanging time and catalepsy time in PD mouse. Our findings suggests that OLE treatment significantly improved postural instability, muscular strength and motor impairment induced by rotenone intoxication.

Reduced activity of some major antioxidant enzymes such as SOD and catalase in rotenone-treated cells has been reported^{44,45}. In our study, we have also observed the decrease in enzymatic activity of SOD and catalase with rotenone intoxication due to increase ROS generation. While dose of 16 and 32 mg/kg bwt OLE administration, increases the enzymatic activity by scavenging ROS. This could be due the formation of intra molecular hydrogen bonding of OLE with free radicals⁴⁶. Stressful environment produces free radicals, which then interact with free oxygen molecules on membrane lipids to produce peroxy radicals, which are responsible for lipid peroxidation⁴⁷. Our research confirms that Rotenone-intoxicated mice had higher MDA levels in the nigrostriatal area, as reported by other⁴⁸ whereas OLE treatment results in decrease in MDA level.

Since TH is a rate limiting enzyme in the synthesis of dopamine⁴⁹, our study also deals with the observation of TH immunoreactivity in SN and ST region. Due to rotenone intoxication, reduced immunoreactivity of TH was found whereas, 16 and 32 mg/kg bwt of OLE showed a significant increase in expression of TH. OLE reversed the loss of TH expression and maintained the TH integrity of nerve terminals. On the basis of neurobehavioral analyses, metabolic data, and TH immunoreactivity it has been observed that 16 and 32 mg/kg bwt dose of OLE are more efficacious than the 8 mg/kg bwt dose of OLE.

Rotenone reduced the production of ATP in dopaminergic neurons to a higher extent than non-dopaminergic neurons by inhibiting complex I⁴⁰. Mitochondrial biogenesis is also influenced by signalling molecules and

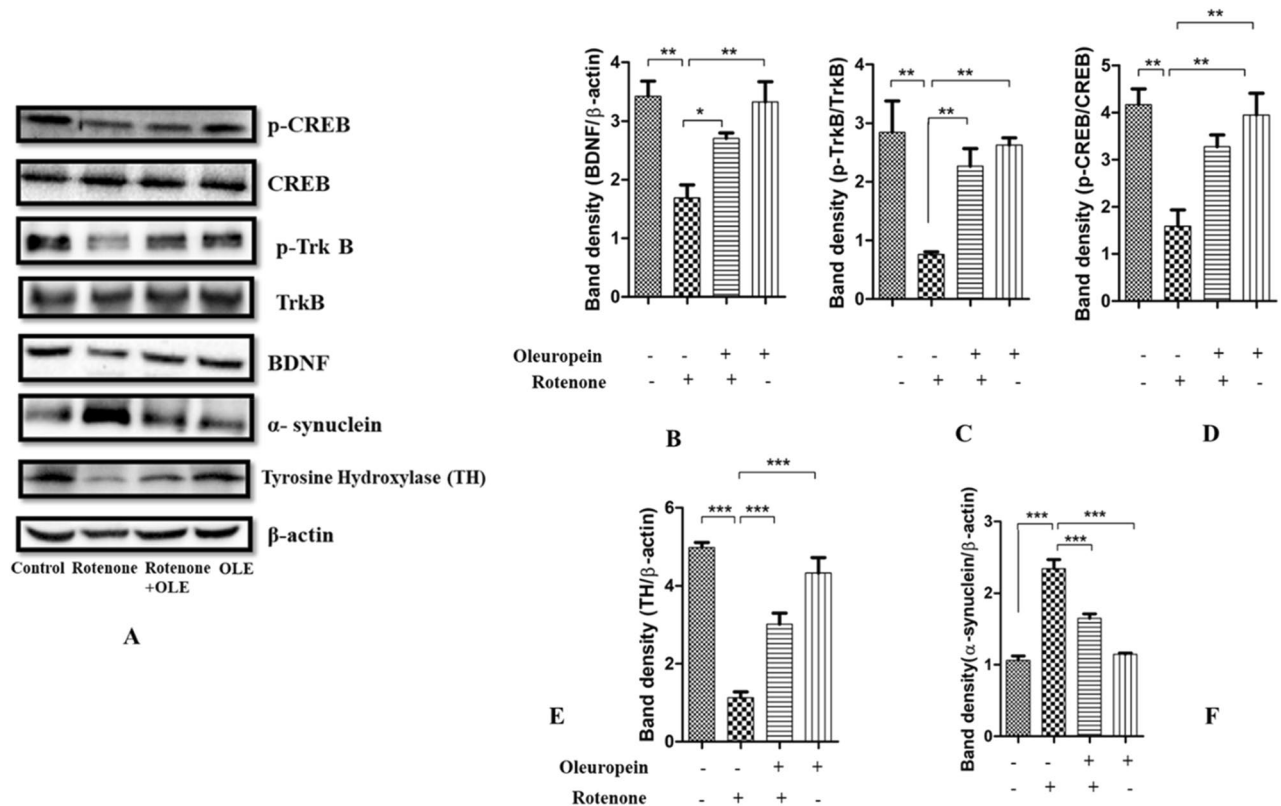


Figure 8. (A–F) This figure shows the relative expression of α -synuclein, TH, p-Trk B, BDNF, p-CREB, in which β -actin acts as a control (A). The lower expression of BDNF (B), p-Trk B (C), CREB (D), TH (E) was observed in case of rotenone-intoxicated mice ($***p < 0.001$) ($**p < 0.01$) respectively. while OLE administered group showed significantly increased expression of TH, CREB, BDNF and p-Trk B and BDNF ($***p < 0.001$) ($**p < 0.01$) respectively. Aggregation of α -synuclein (F) was found to be more in rotenone group ($***p < 0.001$) than control whereas OLE-treated group showed lower aggregation of α -synuclein ($***p < 0.001$). The one-way ANOVA was used to analyse the data, followed by the Newman–Keuls test. The mean \pm SEM ($n = 6$) is used to depict the values.

neurotrophic substances such as BDNF⁵⁰. The effect of BDNF, GDNF, and NGF on oxidative metabolism in mouse brain mitochondria has been investigated *in vitro*^{51,52}. In PD, blocking GSK-3 β activation protects dopaminergic neurons against rotenone-induced toxicity by preventing apoptosis caused by complex I inhibition⁵³. Our observation reinforced the previous evidence by showing the reduced activities of ETS complexes I, complex IV, and complex V due to mitochondrial dysfunction. Aggregation of α -synuclein and increase in oxidative stress must have contributed to the reduced complex activity. This can be linked to the increased GSK3 β activation and Ca^{2+} levels in the cytoplasm. It is therefore hypothesised that the altered activities of the mitochondrial complexes caused by rotenone, prevented the transport of electron between the complexes, which was reduced by the administration of OLE.

TrkB has a high affinity for BDNF, which aids in the survival of Nissl-stained neuronal cells and dopaminergic neurons, as well as preserves dopaminergic connections to the ST⁵⁴. Research has shown that TrkB expression was dramatically decreased in MPTP-induced C57/BL6 mice models of PD⁵⁵. α -Synuclein aggregates interact directly with TrkB receptor which hinders the interaction of BDNF and TrkB. This leads to reduced neurotrophic activities, making DA neurons more vulnerable to degeneration⁵⁶. Hence, α -synuclein-mediated upregulation of TrkB ubiquitination, hindered TrkB axonal trafficking and decreased TrkB protein level⁵⁷. The current study validated the previous concept by demonstrating the decrease in the expression of BDNF and TrkB in the rotenone intoxicated mice model due to the accumulation of α -synuclein. OLE has significantly induced BDNF-TrkB interaction and helps in suppression of α -synuclein pathology. This might be due to the conformational change in TrkB receptor induced by OLE which facilitates the binding of BDNF and TrkB, showing its neuroprotective role.

In several studies, Akt has been found to play a role in cellular signal transduction, as it is activated after binding of TrkB and BDNF^{58,59}. GSK-3 β and α -synuclein interaction results in the disruption of BDNF signalling, which is one of the complex pathways in PD neuropathology^{60,61}. According to Golpich et al., Akt can decrease GSK-3 β activity by phosphorylating ser9 of GSK-3 β which downregulate the series of programmed cell death⁶². Furthermore, aberrant GSK-3 β regulation might result in PD pathophysiological symptoms⁶³. GSK-3 β inhibitors have been found to increase both BDNF mRNA and protein in cultured cortical neurons, suggesting that GSK-3 β activity has a direct effect on neuronal BDNF level^{64,65}. In accordance with previous research, our findings showed the reduction in BDNF and TrkB expression. The p-Akt/Akt ratio and the p-GSK3 β /GSK3 β ratio were both

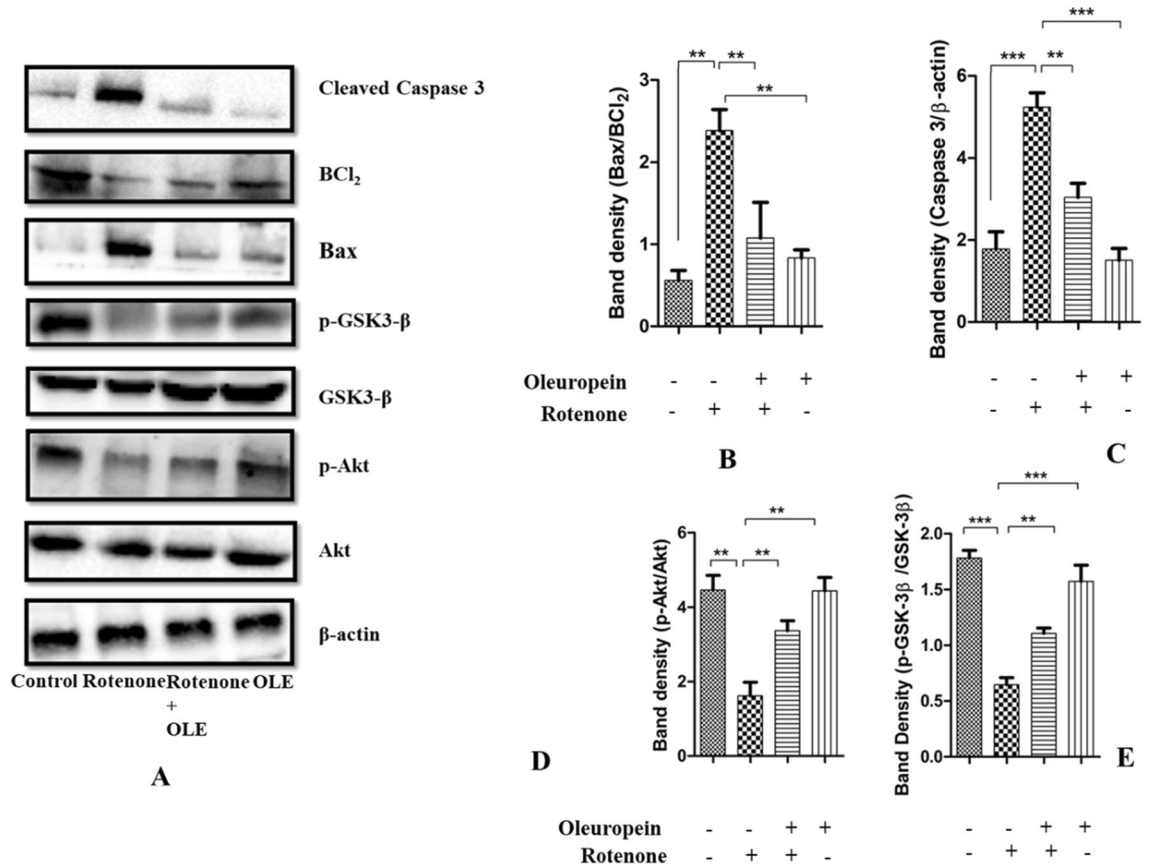
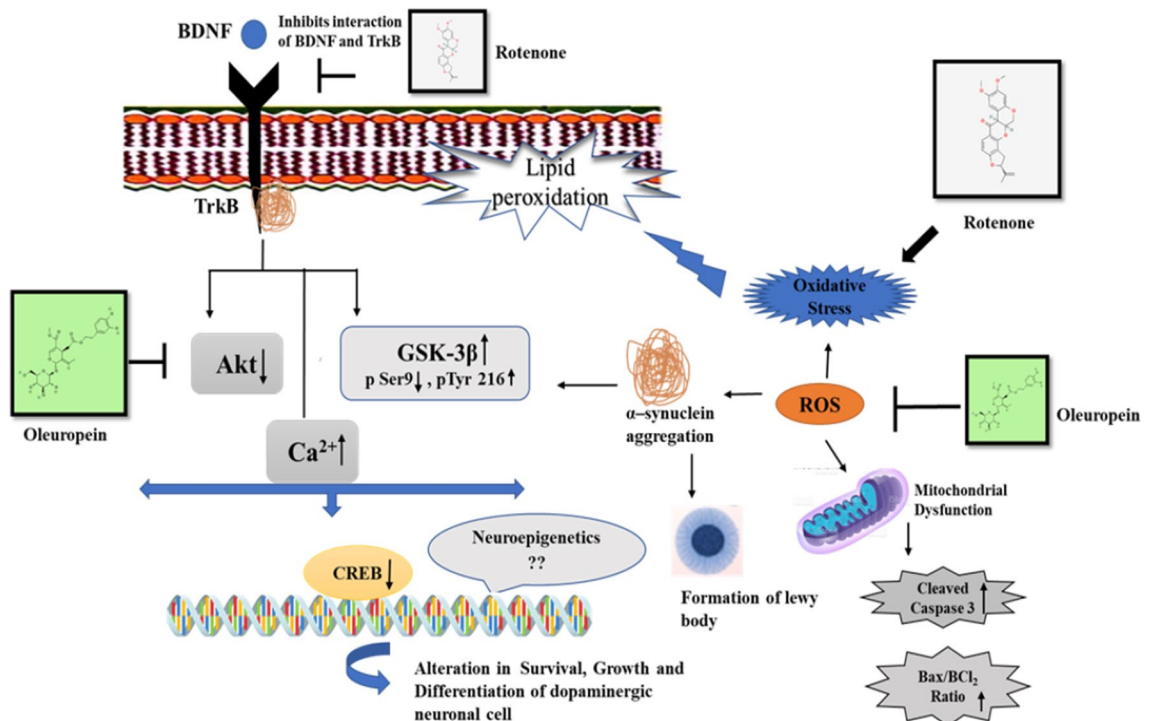


Figure 9. (A–E) Using the Western blotting method and protein densitometry analysis, the relative expression of Bax, Caspase-3, Bcl-2, p-Akt and p-GSK-3β was examined in the SN of mice (A). OLE inhibited the increase in ratio of Bax/BCl₂ (B) and decrease in the expression of cleaved caspase 3 (C). Additionally, phosphorylation of Akt (D) and GSK3β (E) was increased by OLE. The one-way ANOVA was used to analyse the data, followed by the Newman–Keuls test. The mean ± SEM (n = 6) is used to depict the values (**p < 0.01 and ***p < 0.001).



lowered in the rotenone group, whereas they were significantly enhanced in the OLE administered group. The immunohistochemistry technique also proved the previous finding and shows reduced expression of p-GSK3 β in case of rotenone while OLE increased the expression of p-GSK3 β , exhibiting their neuro-survival effect. The BDNF-TrkB interaction and the binding of CREB to the BDNF promoter was seen in the aforementioned data, suggesting that targeting the neuronal survival pathway might be more advantageous for the treatment strategy in the case of PD.

Rangasamy et al. have shown that CREB modulates the expression of TH gene by binding to its promoter and thus the expression of both CREB and TH was shown to be downregulated in PD mouse model^{66,67}. We have also observed the lower expression of p-CREB and TH protein in nigrostriatal region of rotenone induced mouse and higher expression in OLE treated group through Western blotting analysis.

Additionally, the lower levels of CREB phosphorylation may be caused by the inactivation of upstream signalling proteins, resulting in reduced expression of BDNF in the rotenone group. Phosphorylation of CREB and BDNF was significantly reduced by OLE which verified the earlier evidences. The results of our experiment support that CREB is an important modulator of neurotrophic response and neurons have developed several neurotrophic signalling pathways to CREB.

It was observed that mitochondrial dysfunction and ROS overproduction leads to the disturbance in Ca²⁺ homeostasis in case of PD⁶⁸. Ca²⁺, a key second messenger, is hypothesised to modulate some downstream proteins of BDNF in a rapid and localized way⁶⁹. Ca²⁺ binding to α -synuclein speeds up the production of α -synuclein fibrils in vitro, perhaps contributing to PD etiology^{70,71}. In the present study, rotenone administration causes a rise in nigrostriatal Ca²⁺ level, and OLE treatment results in a significant decrease in cytosolic Ca²⁺ level, suggesting a neuroprotective role of OLE to diminish the progression of PD.

Aggregation of α -synuclein has also been found to increase the Bax/Bcl-2 ratio in several in vitro and in vivo studies of PD^{72,73}. However, mitochondrial dysfunction results in upregulation of proapoptotic factor which triggers the activation of caspase 3, leading to the neuronal cell death⁷⁴. Bcl-2 family members can also be activated by BDNF as reported in MPP⁺-induced neuronal cell line SH-SY5Y cells and mouse models⁷⁵. Similarly, our Western blotting experiment revealed a decrease in the ratio of Bax/Bcl-2 and cleaved Caspase3 in the rotenone induced mouse model due to abrupt increase in ROS level that resulted in uncontrolled series of apoptosis. However, OLE treatment has rescued DA neurons from rotenone-induced toxicity by decreasing the ratio of such pro-apoptotic factors markedly.

Therefore, our finding suggests that the regulation of growth and differentiation of neuron is involved in the origin of PD pathogenesis. Hence, it is required to target neuronal survival pathway from the therapeutic point of view in the treatment of PD. Since PD is primarily sporadic, it will be interesting to study these cellular pathways at the epigenetic level so that genetic and environmental factor, both can be explored for deeper understanding of the disease pathogenesis.

Concluding remarks

Our research suggests that OLE can provide potent neuro-survival effect against the key factors of neurodegeneration in PD, like oxidative stress, α -synuclein upregulation, altered Ca²⁺ level, mitochondrial dysfunction, downregulation of neurotrophic factors and apoptosis by regulating BDNF/Akt/CREB signalling. OLE should be studied further at the epigenetic and pre-clinical level as a prospective pharmacological option for amelioration of neurodegeneration in PD.

Dose chase experiment for the analysis of neuroprotective action of OLE

Methods. *Ethical approval.* The institutional animal ethics committee of BHU in Varanasi, India, accepted this study. The experiments were carried out in accordance with the institutional ethical standards, and they were approved by the institutional animal ethics committees (IAECs) of the laboratory animal research at Banaras Hindu University in India (IAECs Approval Reference No. BHU/DoZ/IAEC/2021-2022/031). Animal experiment design, execution, and reporting all according to the ARRIVE guideline. The number of mice used was kept to a minimum. Every attempt was made to reduce animal pain.

Experimental animals. Eight to ten-week-old male Swiss albino mice (25 \pm 5 g) were facilitated by the Institute of Medical Sciences at Banaras Hindu University in India. Mice were acclimatised to laboratory settings with constant light–dark cycles of 12 h for 7 days prior to the commencement of the experiment. All animal experimental protocols were approved by the Animal Ethics Committee of Banaras Hindu University in Varanasi, India.

Experimental designs. The first group had employed as control and the second group was injected with rotenone. The vehicle for the control group was 0.9% normal saline. The third, fourth, and fifth groups was initially administered with intraperitoneal doses of OLE i.e. 8 mg/kg, 16 mg/kg and 32 mg/kg body weight respectively for 7 days and later was simultaneously administered with rotenone for 35 days. The solubility of OLE was in 0.9% normal saline and rotenone was diluted in sunflower oil to a final concentration of 2 mg/ml after being dissolved in chloroform at a 50 \times stock solution. Following the completion of dosage, behavioural parameters was assessed and the mice from each group was sacrificed and their brains was collected by decapitation for biochemical tests and further experimental work.

Reagents and antibodies. Ouropein, Rotenone, acetic acid, Bradford reagent (Himedia), EGTA (Ethylenediamine tetraacetic acid), EDTA (ethylene glycol-bis(β -aminoethyl ether)-*N,N,N',N'*-tetraacetic acid), Tris-buffer, sodium dodecyl sulphate (SDS), paraformaldehyde, sodium chloride, sodium hydroxide, disodium hydrogen

phosphate, sodium dihydrogen phosphate, bovine serum albumin (BSA), ammonium chloride, potassium chloride and reduced nicotinamide adenine dinucleotide phosphate (NADPH) were obtained from Sisco Research Laboratories (SRL, Mumbai, India). Potassium dichromate and hydrogen peroxide (H₂O₂) were purchased from Merck (Darmstadt, Germany). Thiobarbituric acid (TBA), 1,4-diazabicyclo 2.2.2 octane (DABCO), and Griess reagent were obtained from HiMedia (Mumbai, India). Lobachemie, India provided the paraformaldehyde and sodium nitrite. Normal goat serum (NGS) was purchased from Sigma–Aldrich (St. Louis, MO, United States). Primary antibody for Akt (Cat. Ab8805), p-Akt (Cat. Ab81283), Bcl-2 (Cat. GR99542-4) and Ca²⁺ detection kit were acquired from Abcam Life Science, Biogenuix Medsystems Pvt. Ltd. (New Delhi, India), and primary antibodies for p-GSK-3β (Cat. SC81462), p-GSK-3β (Cat. SC373800), TH (Cat. SC25269), α-Synuclein (Cat. SC12767), β-actin (Cat. SC47778), and Bax (Cat. SC6236) were purchased from Santa Cruz Biotechnology (Santa Cruz, CA, United States). BDNF (Cat. PA5-95183), CREB (PA1-850) and Caspase-3 (Cat. PA5-77887) and TrkB (Cat. OST00127W) antibody were purchased from Invitrogen (ThermoFisher Scientific). p-TrkB (Cat. ABN1381) antibody was purchased from merckmillipore (Sigma Aldrich). p-CREB (E-AB-20849) was brought from Elabscience.

Behavioural assessments. The following behavioural tests were carried out to assess the motor impairment in rotenone-induced Parkinsonian mice. The mice were trained for three days before to the commencement of the experiment. The motor research employed a variety of tests, including narrow beam walking tests, hanging and catalepsy test.

Narrow beam walking test. The test was conducted to evaluate motor coordination in mice, which is necessary for maintaining balance while travelling on a narrow beam. The test was carried out to assess the motor coordination of mice, which is essential to maintain balance while travelling on a narrow beam. Animals were originally upskilled to walk on a fixed thin wooden beam 100 cm above the flat surface (L100 cm W1 cm). The time of mice to traverse the beam was noticed, and the experiment was repeated three times⁷⁶.

Catalepsy test. In a standard catalepsy test, mice were placed in an odd position and the time it takes to correct it was recorded and that time was used to gauge the severity of catalepsy. Mice were carefully placed with their forelimbs on the bar and their hindlimbs on the floor. When a mouse lifted its hind limbs off a wooden platform, the degree of catalepsy was measured (3 cm). The mice were acclimated for 3 min, and the test was terminated if the delay exceeded 180 s⁷⁷.

Wire hanging test. This neuromuscular behaviour test was used to check the grip strength of the mice. In this test, mice were positioned on a top of wire cage lid and the cage had been inverted. The mice were then hung upside down on the grid until they lost their grasp and fell. The length of time spent suspended was recorded, and the experiment was repeated three times^{78,79}.

Biochemical assessments

After numerous behavioural indicators were examined, mice were sacrificed by cervical dislocation followed by decapitation with minimal pain. The brains of mice were removed and placed on ice to be used later. Mice brains were dissected under ice cold conditions for biochemical experiments, and SN and striatal tissue were separated and maintained at – 20 °C until the procedures were finished⁸⁰. The tissue was then homogenised in KCl buffer (Tris–HCl 10 mM, NaCl 140 mM, KCl 300 mM, ethylenediaminetetraacetic acid 1 mM, Triton-X. To obtain supernatant, the tissue homogenates were centrifuged for 20 min at 4 °C at 12,000g.

Estimation of level of Malondialdehyde (MDA) through lipid peroxidation assay. The level of MDA was measured through LPO test of nigrostriatal tissue as described in earlier study with few modified steps^{81,82}. Briefly, First, 10% tissue homogenate was mixed with 10% SDS, followed by 20% acetic acid. The reaction mixture was then introduced in 0.8% TBA and kept in a boiling water bath for an hour. After cooling the test mixture and centrifuging the supernatant, the absorbance was measured at 532 nm against a control (μmols of MDA per mg protein were used to measure lipid peroxidation).

Estimation of activity of antioxidant enzymes. Inhibition of mitochondrial complexes, especially complex I by rotenone, can cause oxidative stress and ROS production and also results in reduction of activity of antioxidant enzymes. The catalase activity was assessed using a spectrophotometer to measure the rate of breakdown of its substrate hydrogen peroxide⁸³. To accomplish this, the nigrostriatal tissue was incubated in a boiling water bath for 10 min. with potassium dichromate and acetic acid (1:3), and the OD was measured at 570 nm. The enzyme activity was calculated in nmoles/min/mg protein. NADH was used as a substrate to measure SOD activity⁸⁴. Nitro blue tetrazolium chloride (NBT) reduction was inhibited by an enzyme source based on the difference between reference and experimental OD of the sample. The protein was also approximated using the enzyme source. Finally, the absorbance was measured against a reagent blank at 560 nm. SOD activity was measured in units per mg of protein.

Evaluation of TH in SNpc by immunohistochemical staining. *Tissue processing.* Each group of mice was anaesthetized with pentobarbital, then perfused intracardially with 0.9% saline (chilled) and 4% paraformaldehyde (chilled) produced in 0.1 M phosphate buffered saline (PBS), pH 7.4, before being decapitated. Brains were removed and fixed overnight in 10% paraformaldehyde and then swapped three times a day with

sucrose solution (10%, 20% and 30%) for three consecutive days at 4 °C, before being cryoprotected in a 30% sucrose solution. A cryomicrotome (Leica, Wetzlar, Germany) was used to cut 15 µm thick coronal slices passing through SNpc⁸⁵. The sections were rinsed three times in 0.01 M PBS (pH 7.4) before being blocked for 1 h with 10% NGS in PBS, 0.3% Triton-X 100, and 1% BSA in phosphate-buffered saline with Triton X-100 (PBST). The sections were subsequently treated with a polyclonal anti-mouse antibody against TH, Tyrosine Hydroxylase (TH) antibody (1:1250 dilution). After that, the brain sections were incubated at room temperature with FITC-conjugated secondary antibodies (for use with anti-mouse primary) (2 h). The images were acquired with a fluorescence microscope (Nikon, Thermo Fisher Scientific), and then further processed using ImageJ software (File Version 1.4.3.67) (NIH, United States).

Statistical analysis. Graph Pad Prism software (Version 5.01) was used to analyse the data, which included one-way analysis of variance (ANOVA) and the student–Newman–Keuls test. The results are presented as means with standard deviations (SEM). A p-value of 0.05 or below ($p < 0.05$) was considered statistically significant. At each level, the experiments were repeated three times. For various experimental studies control was used appropriately as per requirements.

Effect of OLE on neuronal survival in rotenone-intoxicated parkinsonian mouse model. *Experimental design.* Mice were divided into four groups, each with six individuals. Group I served as the control group, receiving only 0.9% normal saline. Rotenone was administered to the second group; OLE and rotenone were given to the third; and OLE (16 mg/kg bwt.) alone was given to the fourth group. For the first week, Group-III was given intraperitoneally with OLE as pre-treatment and further co-treated with the dose of rotenone for 35 days. In earlier experimental designs, the rotenone and OLE administration methods were detailed.

Mitochondrial assays. *Isolation of mitochondria.* The nigrostriatal area of the midbrain was homogenised using a solution (pH 7.4) containing 225 mM mannitol, 5 mM HEPES, 75 mM sucrose, 1 mM ethylene glycol tetra acetic acid (EGTA), and 1 mg/ml BSA. The mitochondrial pellet was separated from the mouse brain by differential centrifugation⁸⁶. After isolating the nigrostriatal region of brain, the tissue was homogenized with homogenization buffer. The homogenate was then centrifuged for 30 min. at 4 °C at 2000g. After centrifugation, the supernatant was centrifuged again at 12,000g for 10 min. The mitochondria and synaptosomes were obtained from the pellet produced after the second centrifugation and suspended in homogenising buffer containing digitonin (0.02%). To get a crude mitochondrial fraction, the mixture was again centrifuged for 10 min at 12,000g. Mitochondrial pellets was then rinsed twice with homogenising buffer without BSA or EGTA, and the fraction was resuspended in phosphate buffer (50 mM, pH 7.4). The Bradford test was used to determine the concentration of proteins in all of the samples. The experiments were carried out using 20 µg proteins within 24 h after mitochondrial isolation.

Complex I assay. In our investigation, the testing of complexes I was carried out using the technique of Stojakovic et al.⁸⁷. The catalytic oxidation of NADH to NAD⁺ reduced the cytochrome *c* in this experiment. The reaction mixture was made up of NADH (6 mM in 2 mM glycylglycine buffer), glycylglycine buffer (0.2 M, pH 8.5), and cytochrome *c* (10.5 mM). It was then mixed with 20 µg mitochondrial protein and the absorbance was measured at 550 nm for 2 min. At 340 nm, NADH has an extinction coefficient of 6.22/mM/cm. The activity of the enzymes was measured in nmol NADH oxidized/min/mg protein.

Complex IV assay. The oxidation of reduced cytochrome *c* at 550 nm was used to evaluate Complex IV activity⁸⁸. Potassium ferricyanide, 10 mM phosphate buffer (pH 7.4), reduced cytochrome *c*, and 20 µg mitochondrial protein were added in the reaction mixture. A few crystals of sodium borohydride were added to a solution of oxidised cytochrome *c* (10 mg/ml) to produce reduced cytochrome *c*. The complex IV activity was measured in nmol cytochrome *c* oxidized/min/mg of protein after observing the change in absorbance for around 3 min.

Complex V assay. The quantity of inorganic phosphorus released during ATP to ADP hydrolysis was determined in this test. Sarafian's approach was used to test mitochondrial ATPase⁸⁹. The mitochondrial protein was incubated for 5 min at 30 °C in ATPase buffer (5 mM ATP, 2 mM MgCl₂, and 50 mM Tris HCl, pH 8.5). The reaction mixture was spun at 3000g for 10 min. after 10% TCA was added to it. The results were expressed as nmol inorganic phosphate (Pi) liberated per mg protein per minute.

Determination of Ca²⁺ level by calcium assay. A colorimetric calcium detection kit (Abcam) was used to measure the Ca²⁺ level in the nigrostriatal area of the midbrain. The standards and samples were produced in accordance with the kit instructions. After being washed in cold PBS solution, 50 mg of nigrostriatal tissue was resuspended in 500 µL of Calcium Assay Buffer. Using a tissue grinder, tissue homogenization was done manually on ice. Supernatant was collected after homogenates were centrifuged at 5000 rpm for 5 min at 4 °C. The reaction mixture consisted of 90 µL of Chromogenic Reagent, 50 µL of sample, and 60 µL of Ca²⁺ Assay Buffer, which was incubated in the dark for 10 min⁹⁰.

Western blot (WB) analysis. The nigrostriatal region of a mouse brain was homogenised and agitated for 2 h at 4 °C using lysis buffer (RIPA). To collect the supernatant, the homogenate was centrifuged at 12,000 rpm for 30 min and the Bradford test was used to determine the protein content. The polyacrylamide gels were loaded with the whole protein extract (30–50 µg). After that, PVDF membranes were employed for protein

transblotting, and primary antibodies for TH (1:3300), α -synuclein (1:1000), Bax (1:1000), Bcl-2 (1:800), caspase-3 (1:1000), p-Akt (1:1000), Akt (1:1000), p-GSK-3 β (1:1000), GSK-3 β (1:1000), BDNF (1:1000), Trk-B (1:1500), CREB (1:1000) and β -actin (1:1000) were incubated overnight. The membranes were then incubated with the horseradish peroxidase (HRP-) conjugated secondary antibody for 2 h at room temperature after being washed with TBST and TBS. The Enhanced Chemiluminescence (ECL) technique was used to view the blots, and the relative density of each band was determined in comparison to that of β -actin. Blots were cut prior to hybridisation for different antibodies. Quantity One software (Version 4.6.3) was used to calculate relative density (Windows, Bio-Rad).

Immunohistochemistry (IHC). Prior to cutting the section of the brain, all of the procedures were carried out as described above. Using a cryotome, coronal brain slices of 15 μ m thickness were cut. Tissue sections were washed twice in 0.01 M PBS (pH 7.4) for 2 min, then blocked for 1 h with 10% NGS in PBST and subsequently 1% BSA-PBST. After rinsing the sections in PBS, immunohistochemical staining for α -synuclein (1:500), BDNF(1:500), Trk-B(1:500), and p-GSK3 (1:500), was done according to the usual technique and kept it in 4 °C for 16–18 h. Thereafter, the secondary antibodies, TRITC-conjugated (anti-rabbit) and FITC-conjugated (anti-mouse), were diluted in 1% BSA-PBS and incubated for 2 h at room temperature with the corresponding primary-antibody treated tissue sections. PBS, 1% BSA-PBS, and PBS were used to wash sections at each stage. DABCO was used to mount the pieces on the slides⁸⁵.

Statistical analysis. The data was analysed with GraphPad Prism software (Version 5.01) and a one-way analysis of variance (ANOVA) with the Student–Newman–Keuls test and a Student’s two-tailed t-test. The data is provided as mean \pm standard error of the mean (SEM), with p values less than 0.05 considered statistically significant.

Data availability

Complete Raw data is provided in supplementary information.

Received: 2 August 2022; Accepted: 1 February 2023

Published online: 11 February 2023

References

- DeMaagd, G. & Philip, A. Parkinson’s disease and its management: Part 1: Disease entity, risk factors, pathophysiology, clinical presentation, and diagnosis. *Pharm. Ther.* **40**, 504 (2015).
- Aarsland, D. *et al.* Parkinson disease-associated cognitive impairment. *Nat. Rev. Dis. Primers.* **7**, 47. <https://doi.org/10.1038/s41572-021-00280-3> (2021).
- Rizek, P., Kumar, N. & Jog, M. S. An update on the diagnosis and treatment of Parkinson disease. *CMAJ Can. Med. Assoc. J. journal de l’Association medicale canadienne* **188**, 1157–1165. <https://doi.org/10.1503/cmaj.151179> (2016).
- Kouli, A., Torsney, K. M., Kuan, W.-L., Stoker, T. & Greenland, J. *Parkinson’s Disease: Pathogenesis and Clinical Aspects* 3–26 (Codon Publications, 2018).
- Kilzheimer, A., Hentrich, T., Burkhardt, S. & Schulze-Hentrich, J. M. The challenge and opportunity to diagnose Parkinson’s disease in midlife. *Front. Neurol.* **10**, 1328. <https://doi.org/10.3389/fneur.2019.01328> (2019).
- Cerri, S., Mus, L. & Blandini, F. Parkinson’s disease in women and men: What’s the difference?. *J. Parkinsons Dis.* **9**, 501–515. <https://doi.org/10.3233/jpd-191683> (2019).
- Caviness, J. N. Pathophysiology of Parkinson’s disease behaviour—A view from the network. *Parkinsonism Relat. Disord.* **20**(Suppl 1), S39–43. [https://doi.org/10.1016/s1353-8020\(13\)70012-9](https://doi.org/10.1016/s1353-8020(13)70012-9) (2014).
- Dias, V., Junn, E. & Mouradian, M. M. The role of oxidative stress in Parkinson’s disease. *J. Parkinsons Dis.* **3**, 461–491. <https://doi.org/10.3233/jpd-130230> (2013).
- Taylor, J. M., Main, B. S. & Crack, P. J. Neuroinflammation and oxidative stress: Co-conspirators in the pathology of Parkinson’s disease. *Neurochem. Int.* **62**, 803–819. <https://doi.org/10.1016/j.neuint.2012.12.016> (2013).
- Bathina, S. & Das, U. N. Brain-derived neurotrophic factor and its clinical implications. *Arch. Med. Sci. AMS* **11**, 1164–1178. <https://doi.org/10.5114/aoms.2015.56342> (2015).
- Autry, A. E. & Monteggia, L. M. Brain-derived neurotrophic factor and neuropsychiatric disorders. *Pharmacol. Rev.* **64**, 238–258. <https://doi.org/10.1124/pr.111.005108> (2012).
- Palasz, E. *et al.* BDNF as a promising therapeutic agent in Parkinson’s disease. *Int. J. Mol. Sci.* <https://doi.org/10.3390/ijms21031170> (2020).
- Pradhan, J. *et al.* The role of altered BDNF/TrkB signaling in amyotrophic lateral sclerosis. *Front. Cell. Neurosci.* **13**, 368. <https://doi.org/10.3389/fncel.2019.00368> (2019).
- Hu, Y. S., Long, N., Piginio, G., Brady, S. T. & Lazarov, O. Molecular mechanisms of environmental enrichment: Impairments in Akt/GSK3 β , neurotrophin-3 and CREB signaling. *PLoS ONE* **8**, e64460. <https://doi.org/10.1371/journal.pone.0064460> (2013).
- Kisoh, K. *et al.* Involvement of GSK-3 β phosphorylation through PI3-K/Akt in cerebral ischemia-induced neurogenesis in rats. *Mol. Neurobiol.* **54**, 7917–7927. <https://doi.org/10.1007/s12035-016-0290-8> (2017).
- Zhao, X. *et al.* Baicalein alleviates depression-like behavior in rotenone- induced Parkinson’s disease model in mice through activating the BDNF/TrkB/CREB pathway. *Biomed. Pharmacother. Biomed. Pharmacother.* **140**, 111556. <https://doi.org/10.1016/j.biopha.2021.111556> (2021).
- Jin, W. Regulation of BDNF-TrkB signaling and potential therapeutic strategies for Parkinson’s disease. *J. Clin. Med.* <https://doi.org/10.3390/jcm9010257> (2020).
- Baydyuk, M. & Xu, B. BDNF signaling and survival of striatal neurons. *Front. Cell Neurosci.* **8**, 254. <https://doi.org/10.3389/fncel.2014.00254> (2014).
- Kang, S. S. *et al.* TrkB neurotrophic activities are blocked by α -synuclein, triggering dopaminergic cell death in Parkinson’s disease. *Proc. Natl. Acad. Sci. U.S.A.* **114**, 10773–10778. <https://doi.org/10.1073/pnas.1713969114> (2017).
- Qianqian, C. *et al.* Suppression of abnormal α -synuclein expression by activation of BDNF transcription ameliorates Parkinson’s disease-like pathology. *Mol. Ther. Nucleic Acids* <https://doi.org/10.1016/j.omtn.2022.05.037> (2022).
- Zahra, W. *et al.* Anti-Parkinsonian effect of Mucuna pruriens and Ursolic acid on GSK3 β /Calcium signaling in neuroprotection against Rotenone-induced Parkinsonism. *Phytomed. Plus* **4**, 100343. <https://doi.org/10.1016/j.phyplu.2022.100343> (2022).

22. Muratori, B. G. *et al.* BDNF as a putative target for standardized extract of *Ginkgo biloba*-induced persistence of object recognition memory. *Molecules* **26**, 3326. <https://doi.org/10.3390/molecules26113326> (2021).
23. Exner, N., Lutz, A. K., Haass, C. & Winklhofer, K. F. Mitochondrial dysfunction in Parkinson's disease: Molecular mechanisms and pathophysiological consequences. *EMBO J.* **31**, 3038–3062 (2012).
24. Rcom-H'cheo-Gauthier, A., Goodwin, J. & Pountney, D. L. Interactions between calcium and alpha-synuclein in neurodegeneration. *Biomolecules* **4**, 795–811. <https://doi.org/10.3390/biom4030795> (2014).
25. Almeida, R. D. *et al.* Neuroprotection by BDNF against glutamate-induced apoptotic cell death is mediated by ERK and PI3-kinase pathways. *Cell Death Differ.* **12**, 1329–1343. <https://doi.org/10.1038/sj.cdd.4401662> (2005).
26. Rekha, K. R. & Selvakumar, G. P. Gene expression regulation of Bcl2, Bax and cytochrome-C by geraniol on chronic MPTP/probenecid induced C57BL/6 mice model of Parkinson's disease. *Chem. Biol. Interact.* **217**, 57–66. <https://doi.org/10.1016/j.cb.2014.04.010> (2014).
27. Hollingworth, R. M., Ahammadsahib, K. I., Gadelhak, G. & McLaughlin, J. L. New inhibitors of complex I of the mitochondrial electron transport chain with activity as pesticides. *Biochem. Soc. Trans.* **22**, 230–233. <https://doi.org/10.1042/bst0220230> (1994).
28. Burke, R. E. & O'Malley, K. Axon degeneration in Parkinson's disease. *Exp. Neurol.* **246**, 72–83. <https://doi.org/10.1016/j.expneurol.2012.01.011> (2013).
29. Carrera, I. & Cacabelos, R. Current drugs and potential future neuroprotective compounds for Parkinson's disease. *Curr. Neuropharmacol.* **17**, 295–306. <https://doi.org/10.2174/1570159x17666181127125704> (2019).
30. Singh, S. S. *et al.* Neuroprotective effect of chlorogenic acid on mitochondrial dysfunction-mediated apoptotic death of DA neurons in a Parkinsonian mouse model. *Oxid. Med. Cell. Longev.* **2020**, 6571484. <https://doi.org/10.1155/2020/6571484> (2020).
31. Bucciantini, M., Leri, M., Nardiello, P., Casamenti, F. & Stefani, M. Olive polyphenols: Antioxidant and anti-inflammatory properties. *Antioxidants (Basel, Switzerland)*. <https://doi.org/10.3390/antiox10071044> (2021).
32. Romani, A. *et al.* Health effects of phenolic compounds found in extra-virgin olive oil, by-products, and leaf of *Olea europaea* L. *Nutrients* <https://doi.org/10.3390/nu11081776> (2019).
33. Bulotta, S., Oliverio, M., Russo, D. & Procopio, A. *Natural Products*, vol. 156 3605–3638 (Springer, 2013).
34. Elmazoglu, Z., Ergin, V., Sahin, E., Kayhan, H. & Karasu, C. Oleuropein and rutin protect against 6-OHDA-induced neurotoxicity in PC12 cells through modulation of mitochondrial function and unfolded protein response. *Interdiscip. Toxicol.* **10**, 129–141. <https://doi.org/10.1515/intox-2017-0019> (2017).
35. Zhang, Z. *et al.* Baicalein protects against 6-OHDA-induced neurotoxicity through activation of Keap1/Nrf2/HO-1 and involving PKC α and PI3K/AKT signaling pathways. *J. Agric. Food Chem.* **60**, 8171–8182. <https://doi.org/10.1021/jf301511m> (2012).
36. Badr, A. M. *et al.* Oleuropein reverses repeated corticosterone-induced depressive-like behavior in mice: Evidence of modulating effect on biogenic amines. *Sci. Rep.* **10**, 1–10. <https://doi.org/10.1038/s41598-020-60026-1> (2020).
37. Nicholatos, J. W. *et al.* Nicotine promotes neuron survival and partially protects from Parkinson's disease by suppressing SIRT6. *Acta Neuropathol. Commun.* **6**, 120. <https://doi.org/10.1186/s40478-018-0625-y> (2018).
38. Morrison, R. S. *et al.* Neuronal survival and cell death signaling pathways. *Adv. Exp. Med. Biol.* **513**, 41–86. https://doi.org/10.1007/978-1-4615-0123-7_2 (2002).
39. Akbari, M., Kirkwood, T. B. L. & Bohr, V. A. Mitochondria in the signaling pathways that control longevity and health span. *Ageing Res. Rev.* **54**, 100940. <https://doi.org/10.1016/j.arr.2019.100940> (2019).
40. Rai, S. N. *et al.* *Mucuna pruriens* protects against MPTP intoxicated neuroinflammation in Parkinson's disease through NF- κ B/pAKT signaling pathways. *Front. Aging Neurosci.* **9**, 421. <https://doi.org/10.3389/fnagi.2017.00421> (2017).
41. Miranda, M., Morici, J. F., Zanoni, M. B. & Bekinschtein, P. Brain-derived neurotrophic factor: A key molecule for memory in the healthy and the pathological brain. *Front. Cell Neurosci.* **13**, 363. <https://doi.org/10.3389/fncel.2019.00363> (2019).
42. Ntetsika, T. *et al.* Novel targeted therapies for Parkinson's disease. *Mol. Med.* **27**, 1–20. <https://doi.org/10.1186/s10020-021-00279-2> (2021).
43. Palazzi, L. *et al.* Oleuropein aglycone stabilizes the monomeric α -synuclein and favours the growth of non-toxic aggregates. *Sci. Rep.* **8**, 1–17. <https://doi.org/10.1038/s41598-018-26645-5> (2018).
44. Birla, H. *et al.* *Tinospora cordifolia* suppresses neuroinflammation in Parkinsonian mouse model. *Neuromol. Med.* **21**, 42–53. <https://doi.org/10.1007/s12017-018-08521-7> (2019).
45. Birla, H. *et al.* Unraveling the neuroprotective effect of *Tinospora cordifolia* in a Parkinsonian mouse model through the proteomics approach. *ACS Chem. Neurosci.* **12**, 4319–4335. <https://doi.org/10.1021/acscchemneuro.1c00481> (2021).
46. Bulotta, S. *et al.* Biological activity of oleuropein and its derivatives. *Nat. Prod.* **156**, 3605–3638. https://doi.org/10.1007/978-3-642-22144-6_156 (2013).
47. Shichiri, M. The role of lipid peroxidation in neurological disorders. *J. Clin. Biochem. Nutr.* **54**, 151–160. <https://doi.org/10.3164/jc.14-10> (2014).
48. Sochor, J. *et al.* Automation of methods for determination of lipid peroxidation. *Lipid Peroxid.* <https://doi.org/10.5772/45945> (2012).
49. Ogunruku, O. *et al.* Modulation of dopamine metabolizing enzymes and antioxidant status by *Capsicum annum* Lin in rotenone-intoxicated rat brain. *Toxicol. Rep.* **6**, 795–802. <https://doi.org/10.1016/j.toxrep.2019.07.012> (2019).
50. Mostafa Tork, O., Ahmed Rashed, L., Bakr Sadek, N. & Abdel-Tawab, M. S. Targeting altered mitochondrial biogenesis in the brain of diabetic rats: Potential effect of pioglitazone and exendin-4. *Rep. Biochem. Mol. Biol.* **8**, 287–300 (2019).
51. Markham, A., Bains, R., Franklin, P. & Spedding, M. Changes in mitochondrial function are pivotal in neurodegenerative and psychiatric disorders: How important is BDNF?. *Br. J. Pharmacol.* **171**, 2206–2229. <https://doi.org/10.1111/bph.12531> (2014).
52. Chen, S. D., Wu, C. L., Hwang, W. C. & Yang, D. I. More insight into BDNF against neurodegeneration: Anti-apoptosis, anti-oxidation, and suppression of autophagy. *Int. J. Mol. Sci.* <https://doi.org/10.3390/ijms18030545> (2017).
53. Rajendran, M. & Ramachandran, R. Fisetin protects against rotenone-induced neurotoxicity through signaling pathway. *Front. Biosci. (Elite Ed.)* **11**, 20–28. <https://doi.org/10.2741/e843> (2019).
54. Kim, H. I. *et al.* ERR γ ligand HPB2 upregulates BDNF-TrkB and enhances dopaminergic neuronal phenotype. *Pharmacol. Res.* **165**, 105423. <https://doi.org/10.1016/j.phrs.2021.105423> (2021).
55. Zuo, L. *et al.* 7, 8-dihydroxyflavone ameliorates motor deficits via regulating autophagy in MPTP-induced mouse model of Parkinson's disease. *Cell Death Discov.* **7**(1), 254. <https://doi.org/10.1038/s41420-021-00643-5> (2021).
56. Ma, Z. *et al.* Alpha-synuclein is involved in manganese-induced spatial memory and synaptic plasticity impairments via TrkB/Akt/Fyn-mediated phosphorylation of NMDA receptors. *Cell Death Dis.* **11**, 834. <https://doi.org/10.1038/s41419-020-03051-2> (2020).
57. Bobela, W., Nazeeruddin, S., Knott, G., Aebischer, P. & Schneider, B. L. Modulating the catalytic activity of AMPK has neuroprotective effects against α -synuclein toxicity. *Mol. Neurodegener.* **12**, 80. <https://doi.org/10.1186/s13024-017-0220-x> (2017).
58. Katila, N. *et al.* Metformin lowers α -synuclein phosphorylation and upregulates neurotrophic factor in the MPTP mouse model of Parkinson's disease. *Neuropharmacology* **125**, 396–407. <https://doi.org/10.1016/j.neuropharm.2017.08.015> (2017).
59. Luo, S. *et al.* Akt phosphorylates NQO1 and triggers its degradation, abolishing its antioxidative activities in Parkinson's disease. *J. Neurosci.* **39**, 7291–7305. <https://doi.org/10.1523/jneurosci.0625-19.2019> (2019).
60. Albeely, A. M., Ryan, S. D. & Perreault, M. L. Pathogenic feed-forward mechanisms in Alzheimer's and Parkinson's disease converge on GSK-3. *Brain Plast. (Amsterdam, Netherlands)* **4**, 151–167. <https://doi.org/10.3233/bpl-180078> (2018).
61. Nagahara, A. H. & Tuszynski, M. H. Potential therapeutic uses of BDNF in neurological and psychiatric disorders. *Nat. Rev. Drug Discov.* **10**, 209–219. <https://doi.org/10.1038/nrd3366> (2011).

62. Golpich, M. *et al.* Glycogen synthase kinase-3 beta (GSK-3 β) signaling: Implications for Parkinson's disease. *Pharmacol. Res.* **97**, 16–26. <https://doi.org/10.1016/j.phrs.2015.03.010> (2015).
63. Credle, J. J. *et al.* GSK-3 β dysregulation contributes to parkinson's-like pathophysiology with associated region-specific phosphorylation and accumulation of tau and α -synuclein. *Cell Death Differ.* **22**, 838–851. <https://doi.org/10.1038/cdd.2014.179> (2015).
64. Chuang, D. M., Wang, Z. & Chiu, C. T. GSK-3 as a target for lithium-induced neuroprotection against excitotoxicity in neuronal cultures and animal models of ischemic stroke. *Front. Mol. Neurosci.* **4**, 15. <https://doi.org/10.3389/fnmol.2011.00015> (2011).
65. Cuadrado, A., Kügler, S. & Lastres-Becker, I. Pharmacological targeting of GSK-3 and NRF2 provides neuroprotection in a pre-clinical model of tauopathy. *Redox Biol.* **14**, 522–534. <https://doi.org/10.1016/j.redox.2017.10.010> (2018).
66. Rangasamy, S. B., Dasarathi, S., Pahan, P., Jana, M. & Pahan, K. Low-dose aspirin upregulates tyrosine hydroxylase and increases dopamine production in dopaminergic neurons: Implications for Parkinson's disease. *J. Neuroimmune Pharmacol.* **14**, 173–187. <https://doi.org/10.1007/s11481-018-9808-3> (2019).
67. Saura, C. A. & Cardinaux, J. R. Emerging roles of CREB-regulated transcription coactivators in brain physiology and pathology. *Trends Neurosci.* **40**, 720–733. <https://doi.org/10.1016/j.tins.2017.10.002> (2017).
68. Surmeier, D. J. & Schumacker, P. T. Calcium, bioenergetics, and neuronal vulnerability in Parkinson's disease. *J. Biol. Chem.* **288**, 10736–10741. <https://doi.org/10.1074/jbc.R112.410530> (2013).
69. Lisek, M., Zylinska, L. & Boczek, T. Ketamine and calcium signaling—A crosstalk for neuronal physiology and pathology. *Int. J. Mol. Sci.* <https://doi.org/10.3390/ijms21218410> (2020).
70. Tsigelny, I. F. *et al.* Role of α -synuclein penetration into the membrane in the mechanisms of oligomer pore formation. *FEBS J.* **279**, 1000–1013. <https://doi.org/10.1111/j.1742-4658.2012.08489.x> (2012).
71. Roodveldt, C., Christodoulou, J. & Dobson, C. M. Immunological features of alpha-synuclein in Parkinson's disease. *J. Cell Mol. Med.* **12**, 1820–1829. <https://doi.org/10.1111/j.1582-4934.2008.00450.x> (2008).
72. Ganjam, G. K. *et al.* Mitochondrial damage by α -synuclein causes cell death in human dopaminergic neurons. *Cell Death Dis.* **10**, 865. <https://doi.org/10.1038/s41419-019-2091-2> (2019).
73. Melo, T. Q., van Zomeren, K. C., Ferrari, M. F., Boddeke, H. W. & Copray, J. C. Impairment of mitochondria dynamics by human A53T α -synuclein and rescue by NAP (davunetide) in a cell model for Parkinson's disease. *Exp. Brain Res.* **235**, 731–742. <https://doi.org/10.1007/s00221-016-4836-9> (2017).
74. Haddadi, R., Nayebi, A. M. & Eyvari Brooshghalan, S. Silymarin prevents apoptosis through inhibiting the Bax/caspase-3 expression and suppresses toll like receptor-4 pathway in the SNc of 6-OHDA intoxicated rats. *Biomed. Pharmacother. Biomed. Pharmacother.* **104**, 127–136. <https://doi.org/10.1016/j.biopha.2018.05.020> (2018).
75. Li, C., Zhang, Y., Liu, R. & Mai, Y. Ramelteon ameliorated 1-methyl-4-phenylpyridinium (MPP $^{+}$)-induced neurotoxicity in neuronal cells in a mitochondrial-dependent pathway. *Bioengineered* **12**, 4868–4877. <https://doi.org/10.1080/21655979.2021.1960767> (2021).
76. Luong, T. N., Carlisle, H. J., Southwell, A. & Patterson, P. H. Assessment of motor balance and coordination in mice using the balance beam. *J. Vis. Exp. JoVE.* <https://doi.org/10.3791/2376> (2011).
77. Ishola, I. O. *et al.* Novel action of vinpocetine in the prevention of paraquat-induced parkinsonism in mice: Involvement of oxidative stress and neuroinflammation. *Metab. Brain Dis.* **33**, 1493–1500. <https://doi.org/10.1007/s11011-018-0256-9> (2018).
78. Van, P. *et al.* *The Use of Hanging Wire Tests to Monitor Muscle Strength and Condition Over Time* (TREAT-NMD Neuromuscular Network/Wellstone Muscular Dystrophy Center, 2011).
79. Hoffman, E. *et al.* A modified wire hanging apparatus for small animal muscle function testing. *PLoS Curr.* <https://doi.org/10.1371/currents.md.1e2bec4e78697b7b0ff80ea25a1d38be> (2016).
80. Nunes, G. B. L. *et al.* Behavioral tests and oxidative stress evaluation in mitochondria isolated from the brain and liver of mice treated with riparin A. *Life Sci.* **121**, 57–64. <https://doi.org/10.1016/j.lfs.2014.11.018> (2015).
81. Turgut, G. *et al.* Changes in the levels of MDA and GSH in mice. *Eastern J. Med.* **11**, 7–12 (2006).
82. Malekela, R. S. *et al.* Acute toxicity, antidiarrhoeal and antioxidant activities of methanolic leaf extract of *Baphia macrocalyx* in mice. *Tanzan. J. Sci.* **46**, 216–227 (2020).
83. Shahidi, F. & Ying, Z. Measurement of antioxidant activity. *J. Funct. Foods* **18**, 757–781. <https://doi.org/10.1016/j.jff.2015.01.047> (2015).
84. Weydert, C. J. & Joseph, J. C. Measurement of superoxide dismutase, catalase and glutathione peroxidase in cultured cells and tissue. *Nat. Protoc.* **5**, 51–66. <https://doi.org/10.1038/nprot.2009.197> (2010).
85. Tu, L. *et al.* Free-floating immunostaining of mouse brains. *JOVE J. Vis. Exp.* <https://doi.org/10.3791/62876> (2021).
86. Hubbard, W. B. *et al.* Fractionated mitochondrial magnetic separation for isolation of synaptic mitochondria from brain tissue. *Sci. Rep.* **9**, 1–13. <https://doi.org/10.1038/s41598-019-45568-3> (2019).
87. Stojakovic, A. *et al.* Partial inhibition of mitochondrial complex I ameliorates Alzheimer's disease pathology and cognition in APP/PS1 female mice. *Commun. Biol.* **4**, 1–20. <https://doi.org/10.1038/s42003-020-01584> (2021).
88. Valenti, D. *et al.* Impaired brain mitochondrial bioenergetics in the Ts65Dn mouse model of down syndrome is restored by neonatal treatment with the polyphenol 7, 8-dihydroxyflavone. *Antioxidants* **11**, 62. <https://doi.org/10.3390/antiox11010062> (2021).
89. Sarafian, T. A. *et al.* Impairment of mitochondria in adult mouse brain overexpressing predominantly full-length, N-terminally acetylated human α -synuclein. *PLoS ONE* **8**, e63557. <https://doi.org/10.1371/journal.pone.0063557> (2013).
90. Kumar, N. *et al.* Inhibitor of sarco/endoplasmic reticulum calcium-ATPase impairs multiple steps of paramyxovirus replication. *Front. Microbiol.* **10**, 209. <https://doi.org/10.3389/fmicb.2019.00209> (2019).

Acknowledgements

RS, HB, SSS, WZ, ASR, HD, PK and SS are grateful for the fellowships received through CSIR, DBT, ICMR, UGC, BHU India. There was no additional source of funding for this research.

Author contributions

R.S.: designed, conducted, and authored the paper. H.B., H.D., and S.S.: in conducting behavioural, biochemical, and mitochondrial analyses. W.Z. and P.K.: aided in the preparation of the manuscript. S.S.S. and A.S.R.: helped in performing Western blotting and IHC. S.P.S.: assisted with the research design and experiment supervision.

Competing interests

The authors declare no competing interests.

Additional information

Supplementary Information The online version contains supplementary material available at <https://doi.org/10.1038/s41598-023-29287-4>.

Correspondence and requests for materials should be addressed to S.P.S.

Reprints and permissions information is available at www.nature.com/reprints.

Publisher's note Springer Nature remains neutral with regard to jurisdictional claims in published maps and institutional affiliations.



Open Access This article is licensed under a Creative Commons Attribution 4.0 International License, which permits use, sharing, adaptation, distribution and reproduction in any medium or format, as long as you give appropriate credit to the original author(s) and the source, provide a link to the Creative Commons licence, and indicate if changes were made. The images or other third party material in this article are included in the article's Creative Commons licence, unless indicated otherwise in a credit line to the material. If material is not included in the article's Creative Commons licence and your intended use is not permitted by statutory regulation or exceeds the permitted use, you will need to obtain permission directly from the copyright holder. To view a copy of this licence, visit <http://creativecommons.org/licenses/by/4.0/>.

© The Author(s) 2023